The effect of the annealing temperature on the local distortion of $La_{0.67}Ca_{0.33}MnO_3$ thin films

D. Cao[1], F. Bridges[1], D. C. Worledge[2], C. H. Booth[3], T. Geballe[2]
[(1)]Department of Physics, University of California Santa Cruz, Santa Cruz, CA 95064
[(2)]Department of Applied Physics, Stanford University, Stanford, CA 94305-4090
[(3)]Los Alamos National Laboratory, Los Alamos, NM 87545
(December 1, 1999)

The $La_{1-x}Ca_xMnO_3$ colossal magnetoresistance (CMR) system has been studied extensively. From our previous work, we find there is an important connection between local distortions and magnetism in these materials. Here we report Mn K-edge fluorescence experiments for thin film samples (3000 Å) of $La_{0.67}Ca_{0.33}MnO_3$: as-deposited, and post-annealed at 1000 K and 1200 K. The local distortion is analyzed in terms of three contributions: static, phonon, and an extra, temperature-dependent, polaron term. The polaron distortion is very small for the as-deposited sample and increases with the annealing temperature. In contrast, the static distortion in the samples decreases with the annealing temperature. Although the local structure of the as-deposited sample shows very little temperature dependence, the change in resistivity with temperature is the largest of these three thin film samples. The as-deposited sample also has the highest magnetoresistance (MR), which indicates some other mechanism may also contribute to the transport properties of CMR samples. We also discuss the relationship between local distortion and the magnetization of the sample.

Keywords: CMR, XAFS, thin film, annealing

I. INTRODUCTION

The Double Exchange (DE) mechanism was originally considered to be the main interaction contributing to the colossal magnetoresistance (CMR)[1–3]. In the DE model, if the spins of two neighboring Mn ions are aligned, then an electron will require less energy to hop from one Mn site to another. Consequently, at low temperature, the lattice will have ferromagnetic (FM) order such that the total system (both local and itinerant system) has the lowest energy. Although the DE model can explain many properties of CMR materials, the magnitude of the MR calculated from the DE model is much smaller than the actual measured MR[4]. Millis *et al* suggested that local *JahnTeller* distortions also play an important role in CMR materials, and are needed to explain the large magnitude of the MR[4] in these materials.

Several experiments, with both X-ray Absorption Fine Structure (XAFS)[5,6] and pair-distribution function (PDF) analysis of neutron diffraction data[7,8], have been done to study the local structure of the CMR materials and an important relationship between the local distortions and magnetism in these materials has been found[5,6]. The new experiments investigate the local structure of thin films of $La_{0.67}Ca_{0.33}MnO_3$ (LCMO) to understand more about this relationship.

Transport and magnetization measurements show that the annealing temperature affects the resistivity and the magnetization of these thin film samples considerably. They also show that a huge MR occurs for the films, especially for the as-deposited sample at low temperature. Other experiments find that the non-fully annealed thin film samples are oxygen deficient; the Curie temperature, T_c, the saturated magnetization, M_0, and the resistivity peak temperature, T_{MI}, of the samples increase with annealing temperature, while the resistivity of the samples decreases[9–12]. For the fully annealed thin film sample, T_c and T_{MI} are almost the same as those of the bulk material. It is not yet clear what mechanisms are responsible for suppressing T_c, M_0 and T_{MI}.

XAFS experiments on these thin film samples allow us to observe the local structure around the Mn sites, primarily the local distortion of the Mn-O bonds. This paper focuses on the *changes* in the local structure of CMR thin films that are induced by annealing at different temperatures. These results may also help us to better understand how annealing modifies other sample properties.

Diffraction studies of $LaMnO_3$ and $CaMnO_3$ have been carried out by several groups[13–15]. They show that the Mn-O bonds in $LaMnO_3$ have three different lengths: 1.91, 1.97 and 2.17 Å[14], while in $CaMnO_3$ they are nearly all the same at 1.90 Å[15](variation is within 0.01 Å). Our previous work has compared our XAFS data with the diffraction results, and found that the local structure around the Mn site in LCMO CMR samples is very similar to the average structure determined by the diffraction data. More comparison details are shown in reference 6.

In Sec. II, we provide a brief description of the samples and some experimental details. We present the magnetization and transport property data and our XAFS results in Sec. IV. The conclusions are given in Sec. V.

II. SAMPLES AND EXPERIMENTS

The $La_{0.67}Ca_{0.33}MnO_3$ thin-film samples were deposited on $SrTiO_3$ substrates using PLD; each film is 3000 Å thick. See reference 10 for additional details.

The samples we chose for the XAFS studies were: as-deposited (750 K), annealed at 1000 K and annealed at 1200 K. The annealed samples were held at their respective temperatures for 10 hours in flowing oxygen. The samples were heated and cooled at 2 K per minute.

The XAFS experiment was done on beamline 10-2 at SSRL using Si <220> monochromator crystals and the 13-element Ge detector to collect Mn K-edge fluorescence data. The thin film samples were aligned at ~55.0° with respect to the X-ray beam to make x, y and z axes equivalent, and thus correspond to a powder. This angle comes from the polarization dependence of the photoelectric effect[16]. For each sample, we made four sweeps at each temperature; for two of these sweeps, we rotated the sample by 1.5° in order to find out the position of glitches, which must be removed.

III. MAGNETIZATION AND RESISTIVITY

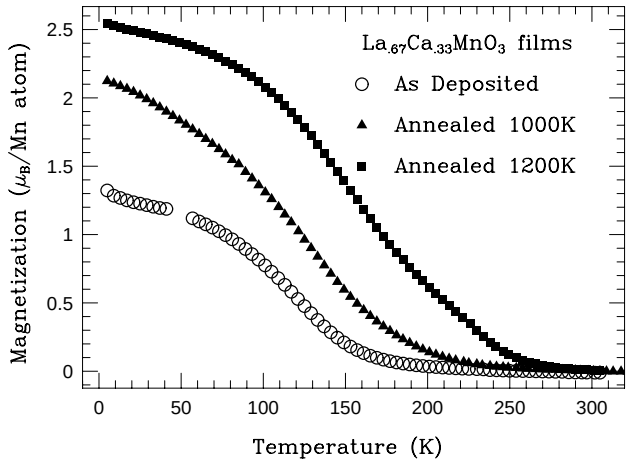

FIG. 1. A plot of magnetization *vs* temperature for $La_{0.67}Ca_{0.33}MnO_3$ thin film samples, with an applied field of H=5000 Oe.

The magnetization *vs* temperature data for these thin film samples are shown in Fig. 1. All samples have broad ferromagnetic-to-paramagnetic phase transitions and T_c increases with the annealing temperature. From these measurements, we extract T_c for these samples (see Table I).

TABLE I. The Curie temperature for each thin film sample.

sample	As-deposited	Annealed 1000K	Annealed 1200K
T_c (K)	164(5)	202(5)	257(5)

The saturated magnetization of the sample increases with annealing temperature. This nicely indicates that at higher annealing temperature, a larger fraction of the sample becomes ferromagnetic in the FM phase at low temperature. Our previous experiments show that the 30% Ca doped LCMO powder sample has a Curie temperature of ~ 260 K[5,6], which is very close to the T_c of the fully annealed thin film sample.

Fig. 2 is a plot of resistivity (ln scale) *vs* temperature for all three samples. We show both the data without field and at 5.5 Tesla. The resistivity decreases with annealing temperature as shown in the figure. At zero field, a large peak is present for the 1000 K annealed sample; the resistivity decreases and the peak moves to higher temperature for the 1200 K annealed sample. There is no metal-to-insulator phase transition for the as-deposited sample; this sample also shows a very large resistivity at low temperature. When the external magnetic field is raised to 5.5 Tesla, the resistivity drops dramatically with magnetic field for the 1000 K and 1200 K annealed samples at temperatures near the resistivity peak, and the resistivity peaks move to higher temperature. For the as-deposited sample, the biggest change in MR occurs at the lowest measuring temperature (70 K). It should also be noted that the peak in resistivity is very close to T_c for the 1200 K annealed sample, but clearly below T_c (over 10 K difference) for the 1000 K annealed sample.

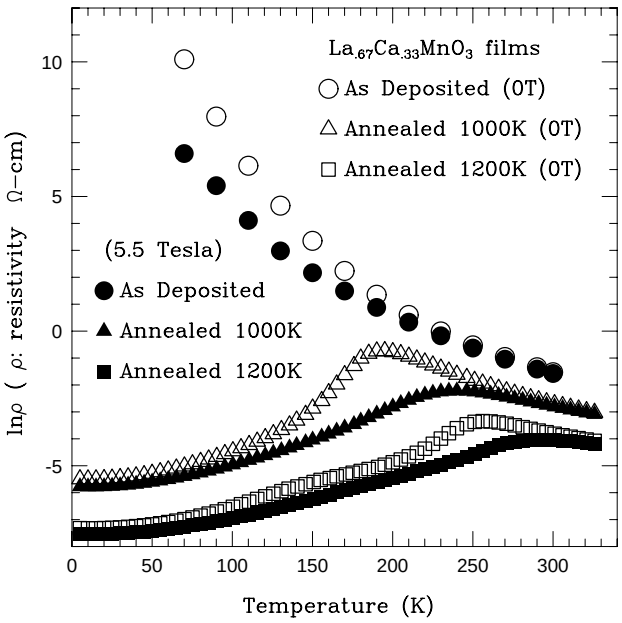

FIG. 2. This plot shows the resistivity data (ln scale) for three thin film samples, with and without magnetic field. The open symbol corresponds to data without field and the solid symbol corresponds to the data with a field of 5.5 T. There is a double peak structure for the 1200 K annealed sample around 150 K, which is just visible in this figure.

Fig. 3 shows MR% (expressed as a percentage) *vs*

temperature data for these samples on a ln scale. Here, we define MR% to be:

$$MR\% = 100\cdot(R_0 - R_H)/R_H$$

where R_0 is the resistivity without magnetic field and R_H is the resistivity with a 5.5 T field.

The magnetoresistivity for these thin films is very large compared to the data for the corresponding powder samples[6]. This is especially true for the as-deposited sample at low temperature—the change of magnetoresistance at 70 K is about 3200%. The maximum MR% is about 1000% for the 1000 K sample and about 250% for the 1200 K sample.

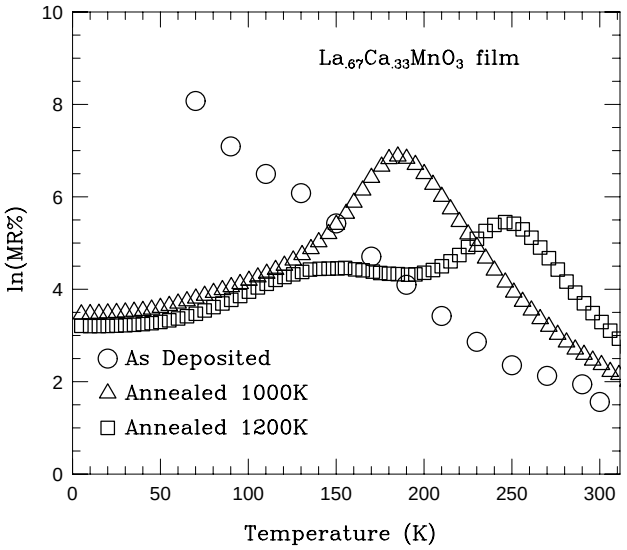

FIG. 3. A plot of MR% (ln scale) *vs* temperature for $La_{0.67}Ca_{0.33}MnO_3$ thin film samples in a field of 5.5 T. The double peak structure for the 1200 K annealed sample is obvious in this plot.

There is a double peak structure for the 1200 K annealed sample clearly visible in Fig. 3. As mentioned earlier, our thin film samples are deposited on $SrTiO_3$ (STO) substrates. When the sample is deposited on STO, some Sr diffuses into the first few hundred Å of the film and changes the stoichiometry of that layer. This Sr diffusion could produce a resistance peak at lower temperature and may be responsible for this extra peak. We chose to use STO substrates instead of $LaAlO_3$ (LAO) substrates, which have no diffusion problem, because the large La $L_I - edge$ XAFS from the substrate would interfere with our Mn K edge XAFS data. Our XAFS data are sensitive to this Sr diffusion layer primarily if we focus on the further neighbor such as Mn-La, Mn-Ca and Mn-Sr. The Mn-O bond distance does not change much between Ca and Sr substitution. Consequently for the Mn-O pair distribution function which is the focus of this paper, we are not very sensitive to Sr in the lower 10% of the film.

IV. XAFS DATA ANALYSIS AND DISCUSSION

We collected all Mn K edge data in transmission mode. The pre-edge absorption (absorptions from other edges) was removed by fitting the data to a Victoreen formula. The photoelectron wave vector k is obtained from $k=\sqrt{2m_e(E-E_0)/h^2}$ and the XAFS function $\chi(k)$ is defined as $\chi(k)=\mu(k)/\mu_0(k)$-1, where $\mu(k)$ is the K-edge absorption coefficient (in this case) and $\mu_0(k)$ is the background function (embedded atom function). After determining the background function, we extracted the k-space data, $k\chi(k)$. An example of such data is shown in Fig. 4. Next we obtain the r-space data from the Fourier Transform (FT) of $k\chi(k)$; fits to the data were carried out in r-space. Some details of these fits are shown later in this paper. See reference 5, 6, 17 for additional details.

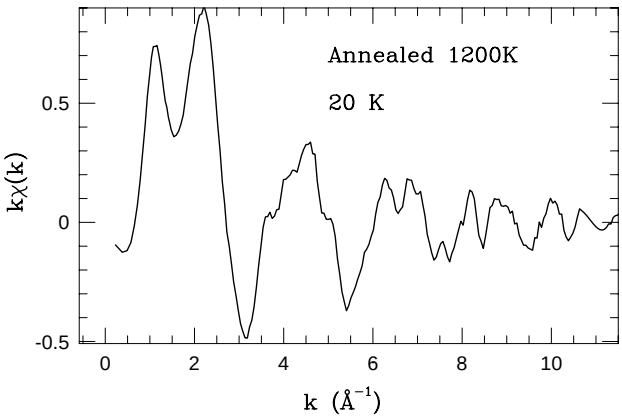

FIG. 4. A plot of the k-space data for the 1200 K annealed sample at 20 K to show the quality of the data. Although there is some noise in the data, the quality is good up to 11 $Å^{-1}$

In Fig. 5, we show the Mn K-edge Fourier transformed (FT) r-space data for all three thin-film samples. In this figure, the position of each peak corresponds to an atom pair; for example, the first peak corresponds to the Mn-O bond (but shifted in position) and the second peak, which is near 3 Å, corresponds to the Mn-La (Mn-Ca) pair. The width, σ, of the pair distribution function is a measure of the local distortions in a shell of neighboring atoms. In XAFS, increased σ leads to a decrease in amplitude of the r-space peak. We obtain some results from this figure immediately. First, the amplitude of the Mn-O peak (the first peak) decreases with increasing temperature. That means there are more distortions in each sample at high temperature. Second, for the higher annealing temperature, the amplitude at low temperature increases and the change of the amplitude with temperature for the Mn-O peak is largest. Most of the distortion observed at 300 K is removed at 20 K for the 1200 K annealed sample. The amount of distortion removed at low temperature is smaller for the 1000 K annealed sample, while most of the distortion in the as-deposited sample is still

present at $T = 20$ K. The amplitude of the r-space data at high temperature (310 K) is almost the same for all three samples; this suggests that the amount of distortion at high temperatures doesn't change very much with the annealing temperature; however it is still clearly less than the local distortion observed previously in $LaMnO_3$ at 300 K[5,6].

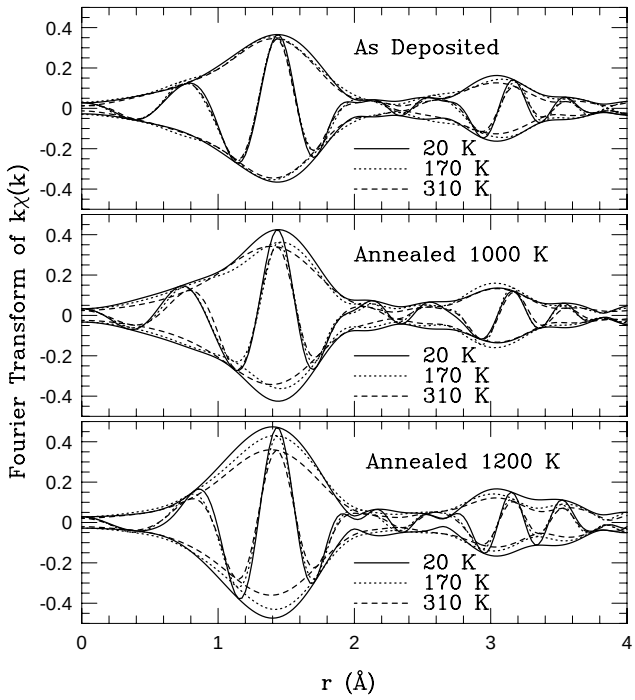

FIG. 5. A comparison of the change in the FT, r-space, data with temperature for the $La_{0.67}Ca_{0.33}MnO_3$ thin-film samples with different annealing temperatures. Top: 750 K anneal (as deposited), middle: 1000 K anneal, bottom: 1200 K anneal. FT range is 3.3–10.5 $Å^{-1}$, with 0.3 $Å^{-1}$ Gaussian broadening. The curve inside the envelope, with a higher frequency, is the real part of the FT (FT_R). The envelope is defined as: $\pm\sqrt{FT_R^2 + FT_I^2}$ where FT_I is the imaginary part of the FT.

Our r-space data were fitted with several Gaussian pair distribution functions. The pair-distribution width, σ(T), was determined from detailed fits to the data, which were carried out using FEFF6 theoretical functions[18] (See Fig. 6). In the fit, S_0^2N was fixed at 4.3. N is the number of nearest neighbours, which is held constant at 6 O neighbors in this case. S_0^2 is an amplitude reduction factor; the main contribution to this factor is the multi-electron process in X-ray absorption. The XAFS oscillations are from one-electron excitations, and S_0^2 is needed to correct for any multi-electron effects. In addition, S_0^2 may also include a correction for small errors in the theoretical calculation. There is an absolute uncertainty in S_0^2 of roughly 10%; small changes in S_0^2 move all the curves up or down in Fig. 6 but do not change the shape or relative position.

The values of σ^2 obtained from the fits provide a measure of the distortion of the Mn-O bond. Different contributions to the broadening add in quadrature and hence σ^2 has the general form:

$$\sigma^2 = \sigma^2_{static} + \sigma^2_{phonons} + \sigma^2_{other-mechanisms}$$

At low temperature, σ^2 is dominated by zero-point motion and some static distortions. For all the manganites, the smallest value for σ is about 0.04 Å; consequently small variations in bond lengths, such as occurring for $CaMnO_3$ are not directly observed in σ. It is surprising that the net distortion of the substituted CMR samples is about as small as that observed for the more ordered $CaMnO_3$ structure at 20 K.

For each temperature 4 traces are analyzed and averaged. The relative errors shown in Fig. 6 are the rms variation of the fit result at each temperature. For the as-deposited sample, σ^2 has a very small change with decreasing temperature; there is a larger change for the 1000 K annealed sample, and an even larger temperature dependence for the 1200 K annealed sample. We also find in Fig. 6 that, at 320 K, σ^2 increases as the annealing temperature is lowered. This indicates that some of the static defects in the as-deposited sample can be removed during the annealing process.

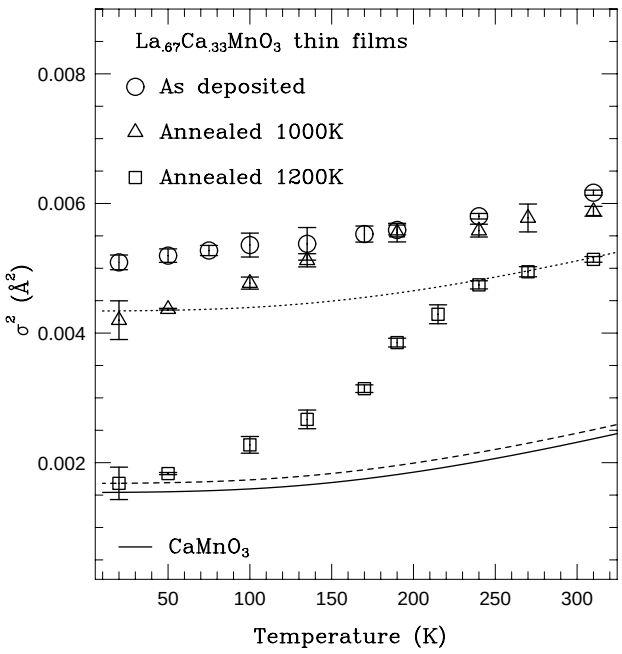

FIG. 6. A plot of σ^2 *vs* temperature for the as-deposited, 1000 K and 1200 K annealed $La_{0.67}Ca_{0.33}MnO_3$ thin-film samples. (Here σ is the pair-distribution width of the Mn-O peak) The solid line is the thermal contribution σ^2_T from $CaMnO_3$, the dashed line corresponds to $\sigma^2_T + \sigma^2_{static}$ and the dotted line is $\sigma^2_T + \sigma^2_{static} + \sigma^2_{FP}$ for the annealed 1200 K sample (see text).

The solid line in Fig. 6 corresponds to the data for

$CaMnO_3$, which has a high Debye temperature (950 K); σ^2 for this sample will be denoted σ_T^2 (The $CaMnO_3$ data we use in this figure are obtained from a powder sample[6]. There might be an uncertainty up to 10% between powder samples and thin film samples since they are in different form and this difference may change the effective value of S_0^2 for the fit process.)

The difference between σ_{data}^2 and σ_T^2 at low temperature is due to a static distortion σ_{static}^2, which is defined as:

$$\sigma_{static}^2 = \sigma_{data}^2(20K) - \sigma_T^2(20K)$$

To estimate this quantity, we shift the solid line vertically until it fits the low temperature data for the 1200 K annealed sample This yields the dashed line in Fig. 6, which is defined to be $\sigma_T^2 + \sigma_{static}^2$. Although σ_{static}^2 is almost zero for the 1200 K annealed sample, it is large for the other samples. We include it here for the 1200 K annealed sample to clarify its definition. The contribution to σ_{data}^2 above the dashed line is attributed to a polaron distortion, where the full (maximum) polaron distortion, σ_{FP}^2, is defined by:

$$\sigma_{FP}^2 = \sigma_{data}^2(300K) - \sigma_T^2(300K) - \sigma_{static}^2$$

We have found in previous work[5,6] that a useful parameter is the distortion removed as T drops below T_c, $\Delta\sigma^2$, which we define below. First, the σ_T^2 curve is shifted vertically (by an amount $\sigma_{FP}^2 + \sigma_{static}^2$) such that it fits the high temperature data. This yields the dotted line shown in Fig. 6 which is $\sigma_T^2 + \sigma_{static}^2 + \sigma_{FP}^2$. This dotted line represents the expected Debye behavior plus static distortion if no polaron distortion were removed upon cooling. We define $\Delta\sigma^2$ as the difference between the dotted line and the data:

$$\Delta\sigma^2 = \sigma_T^2 + \sigma_{FP}^2 + \sigma_{static}^2 - \sigma_{data}^2$$

A similar analysis is carried out for the as deposited sample and the 1000 K annealed sample (corresponding curves for $\sigma_T^2 + \sigma_{static}^2$ and $\sigma_T^2 + \sigma_{static}^2 + \sigma_{FP}^2$ are not shown in Fig. 6). It is also important to point out that the difference between σ^2 for the 1200 K annealed sample and that of $CaMnO_3$ at 20 K is very small, which suggests that the Mn-O local structure of the fully annealed sample can be as ordered as that of $CaMnO_3$ even though it is a doped sample. The same result was obtained for $La_{1-x}Ca_xMnO_3$ CMR powder samples (x = 0.2$\sim$0.5) from our previous experiments[5,6]. The reason for this phenomena for the thin films can be explained as follows: first, the high temperature annealing process appears to remove most of the static defects such as dislocations and vacancies; second, at very low temperatures, there is almost no difference between the two type of Mn sites in the DE model, the electron moves rapidly from one site to another as a time scale fast compared to phonon frequency. Consequently, Jahn-Teller distortions don't have time to form.

For the as-deposited sample, the large MR% occurs when there is a large value for σ^2 at low temperature; this suggests that the distortion in the sample may, in part, be the origin of the unusually large magnetoresistivity in thin-film samples. We have recently observed similar results in our study of Ti and Ga doped LCMO powder samples[19].

In Fig. 7, we plot $\ln\Delta\sigma^2$ *vs* M/M_0. A previous study of $La_{1-x}Ca_xMnO_3$ powder samples showed that there is a linear relationship between $\ln\Delta\sigma^2$ and the magnetization[5,6], which provides evidence that there is a strong connection between the local distortion and magnetism in these materials. The solid squares in Fig. 7 show the linear relationship for a $La_{0.70}Ca_{0.30}MnO_3$ powder sample from our previous work[5,6]. For the thin film samples, there is a similar connection between local distortion and magnetization. For the 1000 K and 1200 K annealed samples, we find a small deviation from a straight line below M/M_0 $\sim$0.3. Since the error of the data in this range ($M/M_0 < 0.3$) is large, it is not clear if this is a real effect or not. The data for the as-deposited sample appear to follow a straight line, but the errors in the difference are too large to draw conclusions. Also, we find that the data for the 1200 K annealed thin-film and the powder sample (both $La_{0.70}Ca_{0.30}MnO_3$) almost overlap each other. This suggests that the local structure of the fully annealed thin-film behaves similarly to that of the corresponding bulk sample.

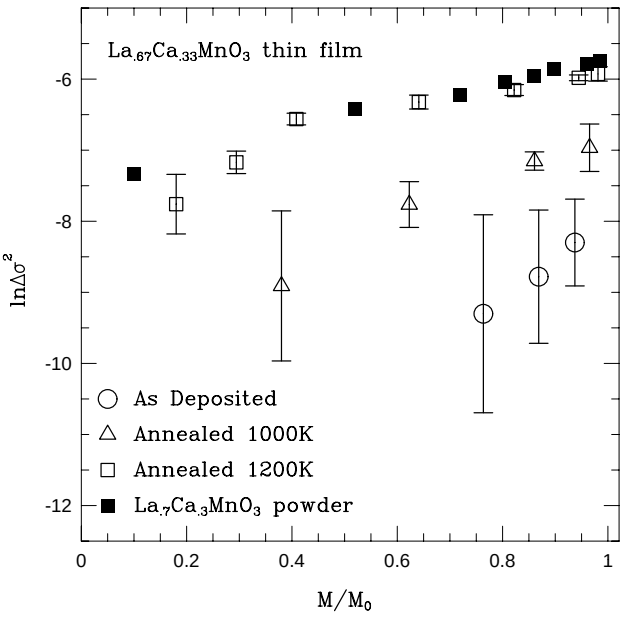

FIG. 7. A plot of $\ln\Delta\sigma^2$ *vs* M/M_0 is presented for the as-deposited, 1000 K, and 1200 K annealed $La_{0.67}Ca_{0.33}MnO_3$ thin-film samples, as well as a $La_{0.70}Ca_{0.30}MnO_3$ powder sample. M is the measured magnetization and M_0 is the saturated magnetization; M/M_0 is the relative magnetization.

In order to see the effect of annealing temperature on

the local distortion more clearly, we plot the distortion contributions, σ^2_{static} and σ^2_{FP}, as a function of annealing temperature in Fig. 8. This figure shows that the static distortion decreases with annealing temperature, while the polaron contribution increases with annealing temperature. This suggests that part of the static distortions observed in the as-deposited sample become dynamic, polaron-like, distortions after annealing, for T > T_c.

It should be noted that although the magnetization only drops by roughly 50% for the as-deposited sample, the σ^2_{FP} contribution becomes much smaller (of order 5%). Consequently, there must be statically distorted regions in the as-deposited sample that are also ferromagnetic. The reduction of the saturated magnetization can arise in several ways. First, because of the inhomogeneous material, small regions may be antiferromagnetic (AF). Second, it has been suggested that the crystal field, particularly in regimes where the inhomogeneity causes a local reduction of the tolerance factor, can result in a low spin Mn ($^4t_{2g}$) configuration with a local 50% decrease in Mn moment[20]. Third, the spins in a small domain may not be exactly parallel. However, to explain the entire decrease in saturated magnetization would require very large canting angles. Fourth, the magnetization vectors of each domain may not be aligned. The number of domain-walls may be important for calculating the resistivity. However, for domains large compared to a unit cell, slightly canted spins within a domain or a lack of alignment of the magnetization of various domains would not lead to a significant decrease in the polaron contribution to the broadening in XAFS. Consequently, the presence of static distortions but essentially no polaron-like contributions in the as-deposited material indicate both a significant fraction of AF material, and the presence of some low spin Mn sites, possibly induced by the disorder (interstitials, vacancies, inhomogeneous Ca concentrations etc.). This disorder must pin the local distortions which would also suppress the electron hopping frequency, thereby reducing the effectiveness of the DE interaction.

All three thin film samples were prepared in the same way, except for the annealing temperature. During the annealing process, part of the static defects in the sample such as vacancies and interstitials can be removed. In addition, the annealing process can also change the amount of oxygen in the sample[9–12]. The sample is slightly oxygen deficient before the annealing process, and oxygen is incorporated during annealing. The fully annealed sample (1200 K) is expected to be fully stoichiometric (similar to the corresponding powder sample). It is well documented that samples without sufficient oxygen can have higher resistivities, a lower resistance peak temperature, a lower T_c and a lower saturated magnetization[9–12]. We have the same trends in our experiments.

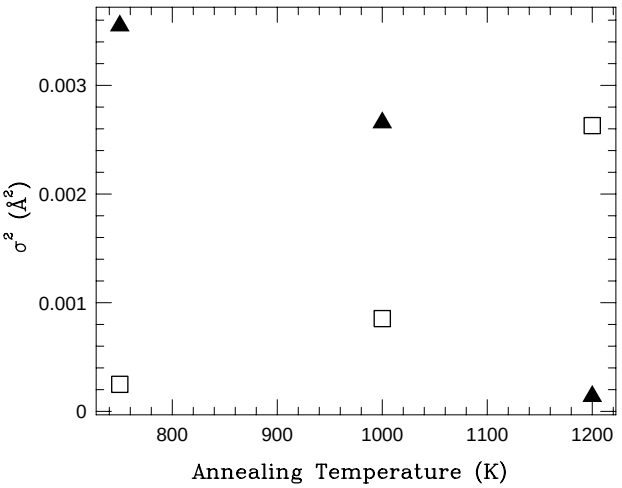

FIG. 8. Static and polaron distortion *vs* annealing temperature for all three thin film samples. The solid triangle symbol represents the static distortion, σ^2_{static}; the open square symbol represents the full-polaron distortion, σ^2_{FP}.

Compared to the 1200 K annealed sample, the samples annealed at lower temperatures have a large decrease in σ^2_{FP} and a large increase in resistivity, while the saturated magnetization changes by less than a factor of two. This suggests that much of the distorted magnetic regions probably do not contribute to the conductivity and that the fraction of conducting material is very low for the as-deposited sample. However, the six order of magnitude increase in resistivity is much larger than the volume reduction of the regions that still have a polaron-like distortion. Consequently, it is likely that percolation also plays a role for transport in the as-deposited sample. Then the magnetic field may play two roles for this sample; it will decrease the resistivity for the conducting pathways that exist at B=0 and may also make some "marginal" pathways become conducting.

V. CONCLUSION

From our analysis, we find that the annealing temperature of the thin films affects the local distortion of the materials appreciably. The large change in resistivity and the small change in local structure with temperature for the as-deposited sample suggest that only small regions are contributing to the resistivity and percolation may play a role. We also find that there is still a strong connection between local distortions, resistivity and magnetism in the fully annealed thin-film materials, which behaves much like a powder sample. For the 1000 K annealed sample, the resistivity and MR peaks are well below T_c. In this case (including the as-deposited sample), the local distortions correlate well with the magnetization, but there is no feature in σ that occurs at the temperature at which the resistivity has a peak.

ACKNOWLEDGMENTS

This work was supported in part by NSF grant DMR9705117. The experiments were performed at SSRL, which is operated by the DOE, Division of Chemical Sciences, and by the NIH, Biomedical Resource Technology Program, Division of Research Resources.

---

[1] C. Zener, Phys. Rev. **82**, 403 (1951).
[2] P. W. Anderson, H. Hasegawa, Phys. Rev. **100**, 675 (1955).
[3] P. G. de Gennes, Phys. Rev. **118**, 141 (1960).
[4] A. J. Millis, P. B. Littlewood, and B. I. Shraiman, Phys. Rev. Lett. **74**, 5144 (1995).
[5] C. H. Booth, F. Bridges, G. H. Kwei, J. M. Lawrence, A. L. Cornelius, and J. J. Neumeier, Phys. Rev. Lett. **80**, 853 (1998).
[6] C. H. Booth, F. Bridges, G. H. Kwei, J. M. Lawrence, A. L. Cornelius, and J. J. Neumeier, Phys. Rev. B **57**, 10440 (1998).
[7] S. J. L. Billinge, R .G. DiFrancesco, G. H. Kwei, J. J. Neumeier, and J. D. Thompson, Phys. Rev. Lett. **77**, 715 (1996).
[8] D. Louca, T. Egami, E. L. Brosha, H. Röder, and A. R. Bishop, Phys. Rev. B **56**, R8475 (1997).
[9] D. C. Worledge, G. Jeffrey Snyder, M. R. Beasley, and T. H. Geballe, J. Appl. Phys. **80**, 5158 (1996).
[10] D. C. Worledge, L. Mieville, T. H. Geballe, J. Appl. Phys. **83**, 5913 (1998).
[11] H. L. Ju, J. Gopalakrishnan, J. L. Peng, Qi Li, G. C. Xiong, T. Venkatesan and R. L. Greene, Phys. Rev. B **51**, 6143 (1995).
[12] N. Malde, P. S. I. P. N. De Silva, A. K. M. Akther Hossain, L. F. Cohen, K. A. Thomas, J. L. MacManus-Driscoll, N. D. Mathur and M. G. Blamire, Solid State Comm. **105**, 643 (1998).
[13] P. Norby, I. G. Krogh Andersen, E. Krogh Andersen, and N. H. Andersen, J. Solid State Chem. **119**, 191 (1995).
[14] J. F. Mitchell, D. N. Argyriou, C. D. Potter, D. G. Hinks, J. D. Jorgensen, and S. D. Bader, Phys. Rev. B **54**, 6172 (1996).
[15] K. R. Poeppelmeier, M. E. Leonowicz, J. C. Scanlon, and J. M. Longo, J. Solid State Chem. **45**, 71 (1982).
[16] R.F. Pettifer, C. Brouder, M. Benfatto, C. R. Natoli, C. Hermes, M. F. Ruiz Lopez, Phys. Rev. B **42**, 37 (1990).
[17] J. J. Rehr, C. H. Booth, F. Bridges, S. I. Zabinsky, Phys. Rev. B **49**, 12347 (1994).
[18] S. I. Zabinsky, A. Ankudinov, J. J. Rehr, R. C. Albers, Phys. Rev. B **52**, 2995 (1995).
[19] D. Cao, F. Bridges, A. P. Ramirez, M. Olapinski, M. A. Subramanian, C. H. Booth, G. Kwei, Unpublished.
[20] T. Geballe, B. Y. Moyzchey, The 5th international workshop in oxide electronics, Dec. 1998, U. of Maryland, Unpublished.